INVESTIGATING CONDITIONS FOR RELAXATION OF SMALL ICY CRATERS IN THE NORTHERN MID-LATITUDES ON MARS. A. B. Cunje[1], A. J. Dombard[1], and E. Z. Noe Dobrea[2] [1]Dept. of Earth & Environmental Sciences, University of Illinois at Chicago, Chicago, IL, 60607 (acunje2@uic.edu), [2]Planetary Science Institute, Moffett Field, CA, 94035.

Introduction: Impact craters can reveal subsurface properties through their morphologies and signs of modification. Here, we explore the population of 1 km diameter and smaller craters in the Green Valley region around the Phoenix landing site to provide insight into the high northern latitudes of Mars. These plains are inferred to host water ice in significant quantities in the near subsurface [1, 2], as well as an ice-rich regolith, as investigated by the Phoenix lander [3]. High water ice abundance values in the range of ~50% by mass have been inferred from epithermal neutron data [1] and landed measurements [4] for the near subsurface, but uncertainties remain with respect to the amount of ice in the subsurface regolith and the thickness of the ice-bearing layer, with suggestions that an excess ice layer could exist below a layer of pore-filled ice within a meter from the surface [5]. This work expands on our previous modeling efforts [6, 7] to investigate the character of the subsurface ice layers at the latitudes of the Phoenix lander and determine conditions that could produce topographic relaxation of appropriate magnitudes and timescales to match the shallow morphologies and modification of the small crater population observed in the Green Valley.

Constraints and findings from crater properties. Examination of the crater population through HiRISE and CTX images around the Phoenix ellipse include evidence for a friable layer inferred to be ice-cemented soils. Most craters below 200-350 m in diameter lack blocky ejecta, while craters larger than this range in the same area do feature blocky ejecta, suggesting larger craters were able to excavate more consolidated material from greater depths [7, 8]. This incompetent layer is estimated to range from 20-35 m deep [8], consistent with SHARAD subsurface radar reflections in the Phoenix landing area, which range from depths of 15-66 m for a dielectric permittivity of water ice and 9-41 m for basalt [9]. Craters larger than 200 m in diameter feature shallow depths and networks of concentric and radial fracture features along with their blocky ejecta, suggesting loss of topography by viscous creep, and retention ages were estimated to be of the order of a few to tens of Myr [8]. The numerous flat craters in the region with no observable topographic relief are effectively palimpsest craters, identified in other studies as boulder halos with suggested infill and inflation processes as responsible for their modification with boulder preservation [10]. In addition to palimpsest craters, several pedestal craters of the order of 1 km and larger are observed in the area, as is the double-layer ejecta (DLE) crater Heimdal with its fluidized ejecta [11]. These may provide insight to the composition of the surface and near subsurface layers as suggested formation processes of the pedestal and DLE crater types respectively include emplacement into ice-rich mantles equivalent in thickness to the crater excavation depth [12], or into pure ice layers tens of meters thick superposed over an ice-cemented silicate regolith [13] that may be mobile and capable of ductile deformation up to 1 km in depth to accommodate crater softening on the surface [14, 15].

Findings of previous modeling studies. From our previous simulations, relaxations of about half the initial crater depth on a timescale of 10 Myr were determined for small 200 m craters emplaced on a 70 m thick ice sheet above a rocky and immobile substrate [6, 7], with cases varying by particulate size and fraction (pure ice or 25% basaltic particulates by volume), surface temperature (185-195 K), and the presence of a welded or free-slip base. Craters 1 km and 600 m in diameter were able to relax fully on similar timescales but only when emplaced into a half-space of pure or particulate ice. These simulations were conducted in light of the finding that a critical threshold of particulate volume fraction exists of ~6%, below which, ice samples flow as pure ice by dislocation creep and grain boundary sliding (GBS), and above which, GBS is impeded [16]. Though complete relaxation was not realized, significant relaxation on relevant timescales was still observed in our simulations driven by the processes of dislocation and diffusion creep, despite GBS flow typically dominating under the relevant temperature and stress conditions [5].

Here we further investigate the conditions necessary to produce relaxation to match observed shallow craters of diameters from 200-1000 m under new layered models thought to best represent the subsurface composition given the crater morphology, ejecta, and radar constraints. Also, we include in some simulations a low viscosity layer of CO_2 ice as a new prospective mechanism to enhance magnitudes and rates of relaxation.

Methods: Following previous modeling works [e.g. 6, 7, 17], we use the MSC.Marc finite element package using a viscoelastic rheology to evaluate the relaxation of Martian craters 200, 600, and 1000 m in diameter in various compositional regimes. Most significantly, we determine that craters 600-1000 m in diameter are unable to relax significantly if the mobile layer thickness is

only a fraction of the crater depth superimposed on a mechanically rigid substrate, so we model a compositional contrast of a pure water ice layer over a stiffer but mobile particulate rich ice (55% particulates by volume) with the boundary at a depth of ~35 m in accordance with the ejecta production transition, SHARAD reflections, and subsurface composition suggested for the formation of pedestal and DLE craters. When implementing our low viscosity CO_2 layer, we convert the lower ~25 m of the 35 m thick pure water ice layer to CO_2 ice, which then forms the new boundary interface with the stiffer substrate. The thickness of the particulate-rich icy substrate is varied relative to the crater diameter to investigate the effect of the mobile layer; "Thick" scenarios have substrate thicknesses equivalent to 2.5 times the crater diameters minus the icy top layer thickness, and "Thin" scenarios are equal to 0.3 times the crater diameters minus the ice layer. A constant surface temperature of 185 K is applied, with a crustal heat flow of 19 mW/m^2 [21]. The creep rheology follows that measured for water ice [16, 18-20]. The creep rheology of CO_2 ice is less well known, so we use preliminary results from recent experiments [22, 23] in a model that gives comparable strain rates to earlier models [24] at stresses of 1 MPa, but has greater strain rates at lower stresses typical of a likely diffusion creep regime.

Results and Discussion: Radial elevation profiles of relaxed craters 1000, 600, and 200 m across are presented (Fig.1). The results of the simulations indicate that relaxation of the small crater population is significant on the relevant timescale of 10 Myr, with the extended mobile substrate able to accommodate additional relaxation and provide a potential source for ejecta if the particulate rich substrate is sufficiently cohesive to produce blocks. A range of thicknesses are used as the depth of mobility for the ice regolith layer is uncertain and likely dependent on porosity with depth or maximum particulate packing fraction [15, 25]. A thickness of 300-400 m of additional mobile substrate is sufficient to allow for significantly enhanced relaxation as seen in the Thin and Thick scenarios for the 1 km and 200 m diameter craters respectively.

While complete crater relaxation to the point of eradication is not achieved in these simulations for the smallest crater size, the significant degree of relaxation on appropriate timescales, especially with regards to the larger crater sizes that would be otherwise immobile if creep is restricted to the thin 35 m ice sheet, suggests that there may be an even more significant reservoir of subsurface ice in the Green Valley region through the extended icy substrate or the existence of a CO_2 ice layer. Viscous relaxation in conjunction with another process such as infill and inflation [10] may be able to reproduce the observed palimpsest crater morphologies for the smaller craters, with localized stresses from relaxation producing fractures in the settled crater fill.

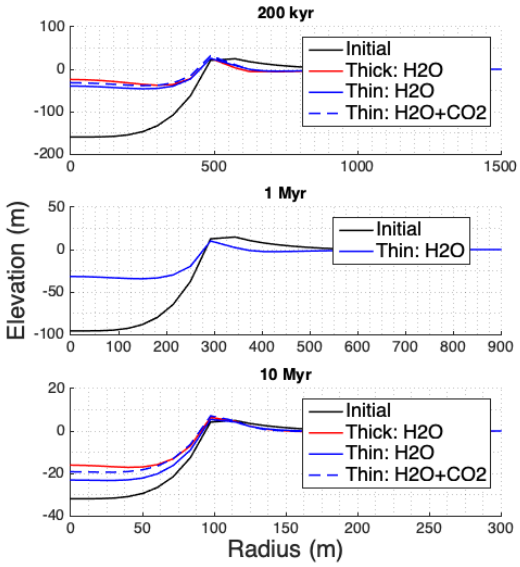

Figure.1: Elevation profiles of relaxed craters of varying diameters: 1000 m (top), 600 m (middle) 200 m (bottom). Black curve: initial shape; red curve: relaxation in Thick regolith substrate; blue curve: relaxation in Thin regolith substrate. Dashed curve: CO_2 layer present.

References: [1] Maurice S. W. et al. (2011) *JGR*, 116. [2] Mellon M. T. et al. (2008) *JGR,* 113. [3] Smith, P.H. (2009) *PhD Dissert.,* U. Arizona.1 [4] Cull S. et al. (2010) *GRL,* 37. [5] Pathare A.V. et al (2018) *Icarus, 301,* 97-116. [6] Cunje A.B. et al (2019) *LPS L,* Abstract #3131. [7] Dombard A. J. & Noe Dobrea E. Z. (2016) *LPS XLVII,* Abstract #1766. [8] Noe Dobrea E. Z. et al. (2019) *Icarus,* in press. [9] Putzig et al. (2014) *JGR:Planets, 119*, 1936-1949. [10] Levy et al. (2018) *JGR:Planets, 123*, 323-334. [11] Heet et al. (2009) *JGR, 114*, E00E04. [12] Kadish S. J. & Head. J.W. (2011) *Icarus, 215,* 34-46. [13] Weiss D. K. & Head J.W. (2013) *GRL*, *40*, 3819–3824. [14] Jankowski D. G., & Squyres S. W. (1992) *Icarus, 100,* 26–39. [15] Mangold N. P. et al. (2002) *Planet. Space Sci., 50,* 385–401. [16] Qi C. et al. (2018) *GRL, 45,* 12757-12765. [17] Dombard A. J. & McKinnon W. B. (2006), *JGR*, 111, E01001. [18] Goldsby D.L. & Kohlstedt D. L. (2001) *JGR, 106,* 11,017-11,030. [19] Kirby S.H. et al. (1987) *J. Phys. C., 48,* suppl., 227-232. [20] Durham W.B. & Stern L.A. (2001) *Annu. Rev. Earth Planet. Sci., 29*, 295–330, [21] Parro L. M. et al. (2017) *Sci. Rep. 7*, 45629. [22] Cross, A.J et al. (2019) *LPSC L,* Abstract #2587. [23] Yamashita, Y. & M. Kato (1997) *GRL, 24 (11)*; 1327-1330. [24] Durham, W.B. et al. (1999) *GRL, 26, (23)*; 3493-3496. [25] Durham, W. B. et al. (2009) *GRL, 36,* L23203.